

Paired Twinning Behavior During Compression of Strongly Basal Textured AZ31 Alloy

Xiong Hanqing¹, Wu Yiping¹, Jia Yuzhen², Xie Shaohui¹, Li Guofeng¹

¹ Changsha University, Changsha 410003, China; ² Bichamp Cutting Technology (Hunan) Co., Ltd, Changsha 410200, China

Abstract: An extruded AZ31 alloy was compressed along the extrusion direction at room temperature. Profuse tensile twins were activated. Paired twins including the connected twin pairs and randomly paired twins (unconnected twins) were studied by a combined analysis of Schmid factor (SF) and strain compatibility factor (m_f). The results show that the nucleation of connected twin pairs preferentially occurs in the neighboring grains with a misorientation of 25°. About 88% of the connected twins have high Schmid factor and about 76% of the connected twins show high strain compatibility factor. The occurrence of connected twin pairs with low values of Schmid factor is well interpreted by their high values of strain compatibility factor. Approximately 22% of the unconnected twin pairs have the strain compatibility factor values of zero.

Key words: AZ31 alloy; twinning; Schmid factor; strain compatibility factor

Magnesium alloys present poor deformability due to the hcp structure^[1-3]. Tensile twinning is an important deformation mode to accommodate *c*-axis strain in Mg alloys, especially those with strong textures, such as extruded and rolled AZ31 alloys^[4-6]. Generally, the occurrence of tensile twins can be predicted by the law of Schmid factor (SF). That is, tensile twins often present high values of SF^[7]. However, some tensile twins with low SF have been found continuously^[8], especially the connected twin pairs in two neighboring grains^[4,5]. The local strain compatibility is important for the twin transfer across neighboring grains. What's more, the investigations of synergetic nucleation of twins and coexistence of orthoposition variants inside one grain need to consider the effect of the local strain compatibility^[4]. Thus, the strain compatibility factor (m_f) has been put forward. The factor m_f explains the relationship between both the two tensile planes and the two tensile directions, which is helpful for the understanding of the low SF behavior among connected twins^[4,9,10]. The factor m_f is defined as follows:

$$m_f = \cos\alpha \cdot \cos\beta \quad (1)$$

where α is angle between the twin plane normal, β is angle

between the twin shear directions. m_f is in the range of $[-1, 1]$, analogous to SF which is in a range of $[-0.5, 0.5]$. If $m_f=1$, it indicates complete strain compatibility over the boundary, and paired twins easily form across the boundary. If $m_f=0$, it indicates that the shear is independent in the neighboring grains. And $m_f=-1$ appears when the shear is exactly opposite to each other.

An extruded AZ31 alloy was compressed along the extrusion direction, and it was found that the distribution of connected twin pairs have high m_f values, and the distribution of unconnected twin pairs is spread over lower m_f values^[11]. In this research, we focused on a detailed analysis of the connected twin pairs and randomly paired twins formed in an extruded AZ31 alloy during compression, including calculations of SF, m_f , misorientation distribution of neighboring grains, etc. The aim is to illustrate the combined effects of SF and m_f on the occurrence of twin pairs in the studied alloy.

1 Experiment

The studied material was an extruded AZ31 rod with a diameter of 30 mm. Compression samples with a dimension of

Received date: February 10, 2019

Foundation item: Changsha University Talent Introduction Project (50800-92808)

Corresponding author: Wu Yiping, Ph. D., Lecturer, Department of Mechanical and Electrical Engineering, Changsha University, Changsha 410003, P. R. China, Tel: 0086-731-84261359, E-mail: wuyipingjia@126.com

Copyright © 2020, Northwest Institute for Nonferrous Metal Research. Published by Science Press. All rights reserved.

Φ8 mm×12 mm were cut from the rod along the extrusion direction (ED). Before compression, the interface between the specimen and the crosshead was lubricated with graphite to reduce friction. Compression tests were conducted on an Instron 30 kN 5567 test machine at a crosshead speed of 1 mm/min at room temperature along ED. One sample was compressed to fracture. Samples with a 2% true compression strain were chosen for the study of twin pairs.

After compression, the compressed samples were cut into halves along the compression direction. The middle position of the cutting plane was prepared for optical microstructure (OM) and electron backscatter diffraction (EBSD) observations to study the twinning behavior. The optical microstructures were examined by Olympus DP 71 optical microscope. The average grain size was obtained by the mean linear intercept method. EBSD maps were obtained on a Leo 1530 field emission gun-scanning electron microscope (FEG-SEM). HKL commercial software (CHANNEL 5) was used to determine the micro-textures.

2 Results and Discussion

2.1 Microstructure and EBSD results

Fig.1a was observed from the longitudinal section of the extruded AZ31 alloy, which displays a reasonably uniform microstructure of equiaxed grains with an average size of ~8 μm. Peculiarly, two long elongated grains and two extra-large equiaxed grains are observed. The extrusions often exhibit a bimodal grain structure which consists of large, elongated, and unrecrystallized “grains” surrounded by newly formed recrystallized grains. Those elongated grains have been suggested to arise from previous unextruded structures that are survived in DRX^[12]. Fig.1b shows that extensive twins occur in the alloy with 2% compression strain. Twins are formed in almost every grain, and some parallel twins are formed in elongated grains.

Fig.2 presents the EBSD results of the extruded alloy and the 2% compressed alloy. In EBSD orientation maps (Fig.2a, 2b), the large angle grain boundary (>15°) is highlighted by

black line and {10 $\bar{1}$ 2} twin boundary (86°±5°<12 $\bar{1}$ 0>) is highlighted by red line. As shown in Fig.2a, equiaxed grains dominate the microstructure of the extruded alloy. The corresponding texture of the extruded alloy is presented in inverse pole figure (IPF) shown in Fig.2c. The extruded alloy has a strong fiber texture with *c*-axes aligned perpendicularly to ED, which enables the occurrence of a large number of tensile twins when compression is performed along ED. This has been proved in Fig.2b. No matter the size of grain is big or small, tensile twins are formed inside. Fig.2d indicates that tensile twins have reoriented *c*-axes by ~90°, forming a texture component of <0001>∥ED. Meantime, the texture

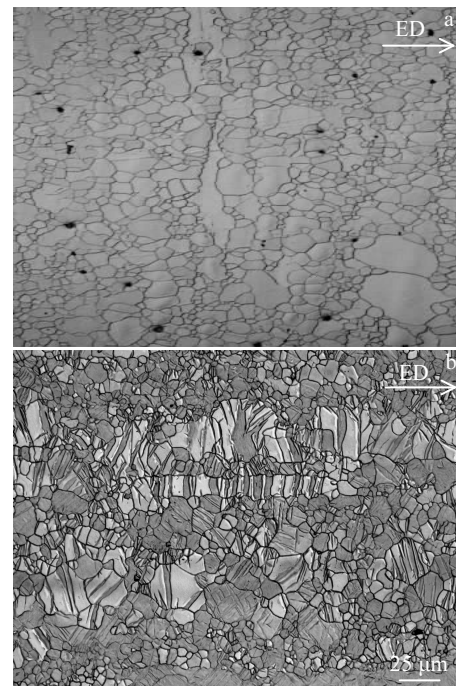


Fig.1 Microstructures of the extruded AZ31 alloy (a) and 2% strain compressed alloy (b)

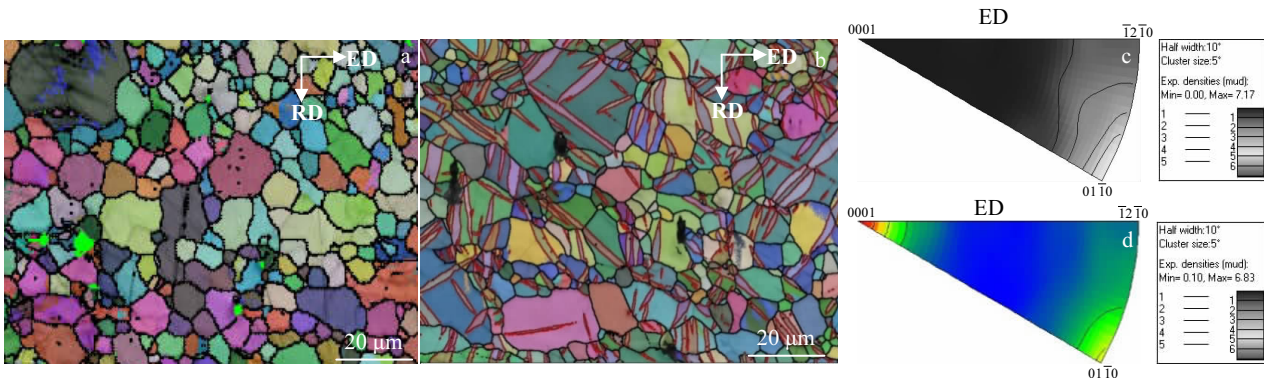


Fig.2 EBSD orientation maps (a, b) and inverse pole figures (IPFs) (c, d) of the extruded AZ31 alloy (a, c) and the 2% compressed alloy (b, d)

component of $\langle 10\bar{1}0 \rangle$ still remains in the compressed alloy.

The typical extrusion texture oriented basal planes are evenly distributed around a plane perpendicular to ED^[13-15]. In some cases of extrusion of Mg alloys, the texture intensities can be distributed homogeneously between the $\langle 10\bar{1}0 \rangle$ and the $\langle 11\bar{2}0 \rangle$ poles. This texture corresponds to the microstructure in which the elongated unrecrystallized grains disappear and grain growth occurs, which are typical recrystallization behavior of Mg alloys^[13]. In the present paper, as shown in Fig.2c, the extruded alloy shows a texture component of $\langle 10\bar{1}0 \rangle // ED$, slightly spreading over the $\langle 11\bar{2}0 \rangle$ pole.

In Mg alloys, basal $\{0001\}$, prismatic $\{10\bar{1}0\}$ and pyramidal $\{10\bar{1}1\} + \{11\bar{2}2\}$ are the common slip systems for deformation and they all contain the same close-packed direction $\langle 11\bar{2}0 \rangle$. But the critical resolved stress (CRSS) for slip in the basal plane is about two orders of magnitude lower than that of the other two^[16]. Therefore, the basal slip system is responsible for most of the long-elongated grains shown in the as-extruded structure. It also means that these grains are favorably oriented to accommodate extrusion strains without the occurrence of twinning and latent hardening during extrusion. Hence, these grains do not have large enough storage plastic energy to trigger recrystallization. Another explanation is reported that the long-elongated grains show a preference for the $\langle 10\bar{1}0 \rangle$ direction parallel to the ED, such as in the extruded ZK60 alloys^[17].

2.2 SF and m_f calculations

Fig.3 further shows another EBSD map of the 2% compressed alloy. The scale in the right-bottom corner of the map presents the continuous change of color with increasing

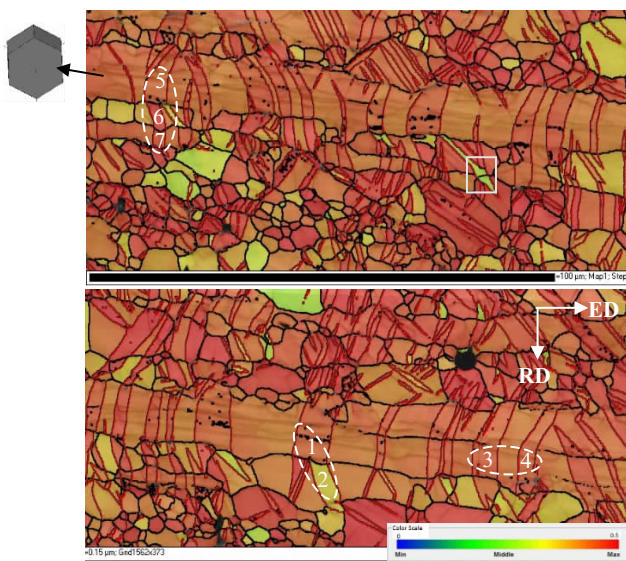


Fig.3 EBSD maps of connected twin pairs and unconnected twin pairs in the 2% compressed alloy

the SF of tensile twin. As shown, many tensile twins are formed in grains with high SF values after compression. As shown by the arrow, the elongated grain aligns its cell crystal with $\langle 10\bar{1}0 \rangle // ED$ and many parallel twins are formed inside after compression. Three examples of common paired twins during the analysis of twinning behavior including connected twins (twins 1 and 2, a T+T event), unconnected twins (twins 3 and 4) and twin chain (twins 5, 6 and 7) are marked in Fig.3. In this study, 50 connected twin pairs and 50 unconnected twin pairs are picked for SF and m_f calculations.

Fig.4a indicates the SF distribution of all tensile twins in Fig.3. About 86% (relative frequency) of tensile twins have a SF in a range of 0.4~0.5. Fig.4b shows the SF distribution of 50 connected twin pairs at grain boundaries. Approximate 88% (relative frequency) of the connected twins present SF values higher than 0.4. Thus, the SF law can explain the occurrence of tensile twins in most cases.

The misorientation distribution between 50 pairs of connected twins and related neighboring grains is further checked, and the results are given in Fig.5a. As shown in Fig.5a, the popular misorientation range of the neighboring grains (black bars) is $10^\circ \sim 35^\circ$, and thereinto, the misorientation of 25° is the optimal location for the nucleation of connected twin pairs. The misorientation of the connected twin pairs is distributed in a similar trend (red bars). These results obtained here coincide

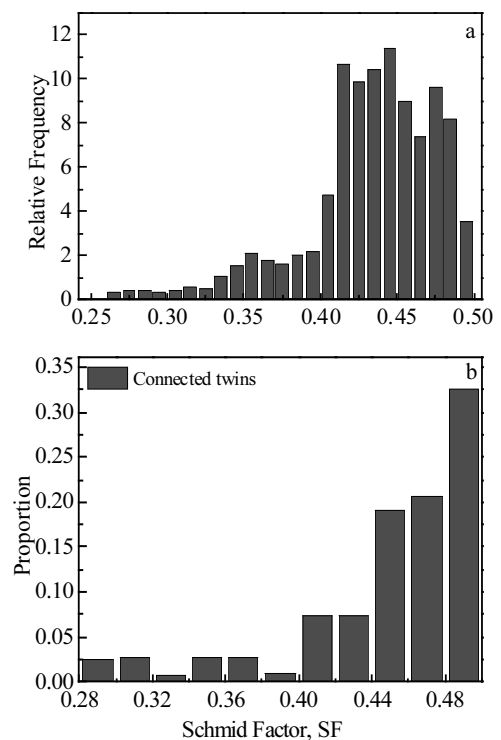


Fig.4 SF distribution of all tensile twins (a) and 50 connected paired twins (b) in Fig.3

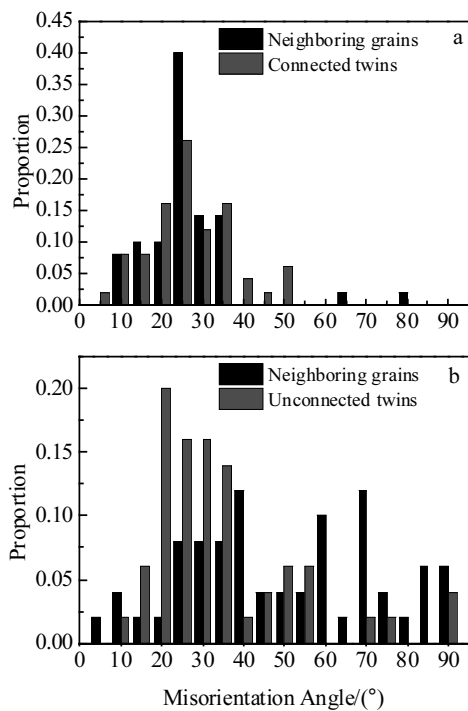


Fig.5 Misorientation distribution between connected twin pairs and related grains (a) and between randomly paired twins and related grains (b)

with the findings of other studies^[11,18,19]. A recent simulation result indicates that the stress concentration along the boundary with low misorientation can activate the occurrence of twin pairs^[18]. Tensile twins are prone to form connected pairs along the grain boundary with small misorientation. With increasing the misorientation, the possibility becomes less^[19]. Twinning is most likely to occur cross boundaries with a misorientation of about 23° in the compression of extruded AZ31 alloy^[11].

The misorientation distribution between 50 pairs of unconnected twins and related unconnected grains is also presented in Fig.5b. Compared with Fig.5a, the distribution is more random. The misorientations of unconnected twins are mostly distributed in two ranges of 15°~35° and 45°~55°. And the misorientation of the unconnected grains is irregularly distributed.

Fig.6 shows the m_f distribution of the connected twin pairs and unconnected twin pairs. As shown, ~76% of the connected twins display m_f values greater than 0.6. For randomly paired twins, only ~26% presents m_f values higher than 0.6, and ~22% shows an m_f equal to zero. This result supports the idea that the transfer of twinning event from one grain into its neighboring grains is accomplished through a stress relaxation event. Thereby, the new twin shows good strain compatibility with the “trigger” twin. It was reported that in the cases of

23% connected twin pairs in the neighboring grains, the strain compatibility factor m_f even possesses more significance than SF for the occurrence^[4].

A pair of green twins with SF values lower than 0.4 are shown in a yellow rectangle in Fig.3, and the area is magnified in Fig.7a. The matrix is marked as M1 and M2, and the twins are shortened to T1, T2, T3 and T4, separately. Their corresponding crystal cells are also given in Fig.7a. SF values of T2 in the grain M1 and T3 in the grain M2 are 0.29 and 0.28, respectively. The misorientations between T2 and T3, M1 and M2 are 13° and 14°, respectively. The calculation of m_f value of the connected twin pair (T2+T3) is illustrated in Fig.7b and 7c. As depicted in the $\{10\bar{1}2\}$ twin plane pole figure (Fig.7b) and $\langle 10\bar{1}1 \rangle$ twin direction pole figure (Fig.7c), the misorientation between the twin plane normals of T2 and T3 is 9.44°, and the misorientation between the twin directions is 14.56°. Thus, m_f for T2 and T3 is equal to 0.95. Thus, despite SF values of both T2 and T3 are lower than 0.4, the high m_f value of ~0.95 ensures the formation of the connected twin pairs (T2+T3).

The nucleation of a T+T event actually can be affected by other unidentified factors, such as grain boundary inclination in three-dimension space, subsurface grain disorientation relationship, pre-existed dislocations, dislocation boundary interactions, differences between global and local stress state, etc^[20,21]. For the present studied alloy, the initial texture replaces most grains in the optimal orientation for the formation of tensile twins during compression. Meantime, the extruded alloy was only subjected to a small true compression strain. Hence, the strain along c -axes can be primarily accomplished by twinning. Thus, during SF and m_f analyses of twin pairs, some impacts, such as the pre-existed dislocations, can be ignored and the results can be concluded simply and purely. According to the above SF and m_f analyzing results, the strain compatibility factor successfully explains the case of the formation of connected twin pairs with low SF in Fig.3.

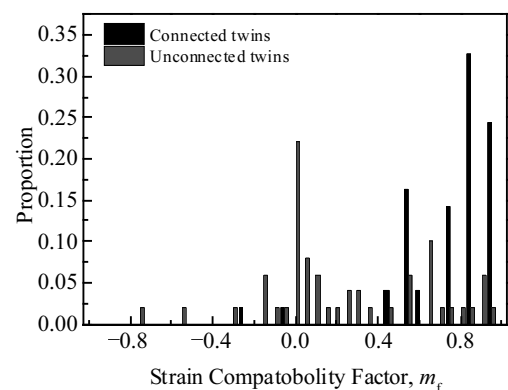


Fig.6 Strain compatibility factor distribution of twin pairs

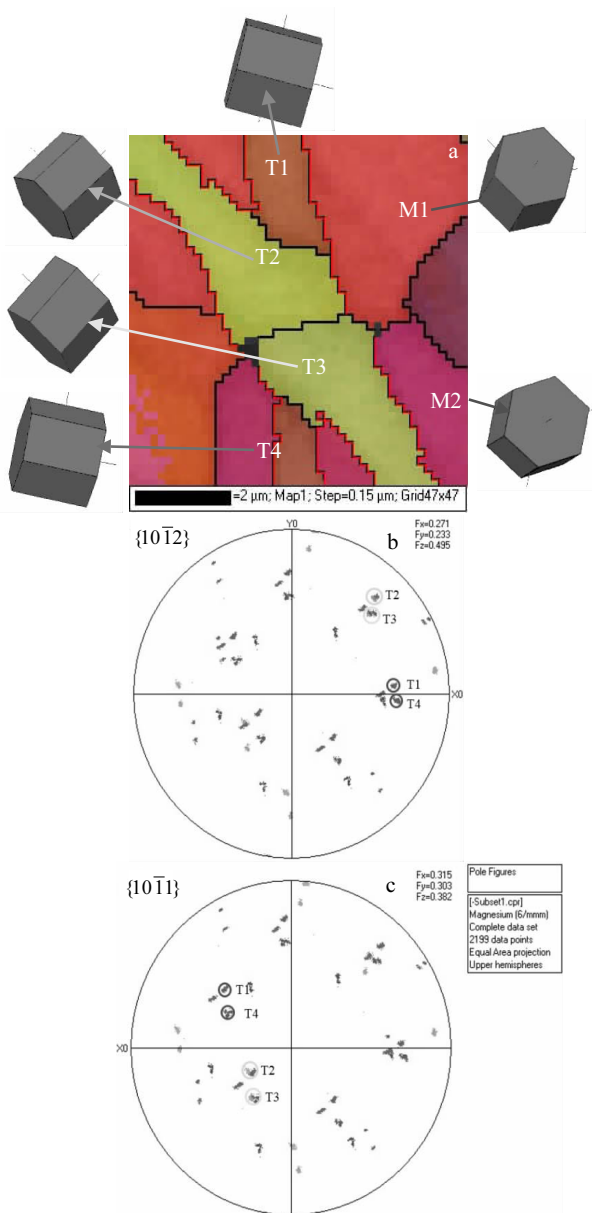


Fig.7 Four twins (T1, T2, T3 and T4) in the parent grains M1 and M2 (a); pole figures of $\{10\bar{1}2\}$ twin plane (b) and $\langle 10\bar{1}1 \rangle$ twin direction (c) in Fig.7a

3 Conclusions

1) The main texture component of the alloy is changed from the $\langle 0001 \rangle \perp ED$ to $\langle 0001 \rangle // ED$ after 2% strain compression along ED because of the profuse occurrence of tensile twins.

2) The most popular location for the formation of connected twin pairs is along the grain boundaries with a misorientation of 25° . $\sim 88\%$ of connected twins have Schmid factor values

in a range of 0.4~0.5. $\sim 76\%$ of connected twins have the strain compatibility factor values in a range of 0.6~1.0. The strain compatibility factor can well explain the formation of connected twin pairs with low Schmid factor in the studied alloy.

3) The distribution of the strain compatibility of the unconnected twin pairs is random, most concentrated around zero.

References

- Liu Qing. *Acta Metallurgica Sinica*[J], 2010, 46(11): 1458 (in Chinese)
- Peng Jian, Pan Fusheng, Ding Peidao et al. *Rare Metal Materials and Engineering*[J], 2009, 38(4): 655 (in Chinese)
- Liu Huaqiang, Tang Di, Hu Shuiping et al. *Acta Metallurgica Sinica*[J], 2013, 49(7): 1372 (in Chinese)
- Guo C F, Xin R L, Xu J B et al. *Materials & Design*[J], 2015, 76: 71
- Guo C F, Xin R L, Ding C H et al. *Materials Science and Engineering A*[J], 2014, 609: 92
- Song Guangsheng, Chen Qiangqiang, Xu Yong et al. *Rare Metal Materials & Engineering*[J], 2016, 45(12): 3186 (in Chinese)
- Pei Y, Godfrey A, Jiang J et al. *Materials Science and Engineering A*[J], 2012, 550: 138
- Barrett C D, Kadiri H El, Tschopp M A. *Journal of the Mechanics and Physics of Solids*[J], 2012, 60(12): 2084
- Shi Z Z, Zhang Y D, Wagner F et al. *Acta Materialia*[J], 2015, 83: 17
- Shi Z Z. *Journal of Alloys & Compounds*[J], 2017, 716: 128
- Barnett M R, Nave M D, Ghaderi A. *Acta Materialia*[J], 2012, 60(4): 1433
- Bohlen J, Yi S B, Swiostek J et al. *Scripta Materialia*[J], 2005, 53(2): 259
- Bohlen J, Yi S, Letzig D et al. *Materials Science and Engineering A*[J], 2010, 527(26): 7092
- Xu S W, Zheng M Y, Kamado S et al. *Materials Science & Engineering A*[J], 2012, 549: 60
- Elsayed F R, Sasaki T T, Ohkubo T et al. *Materials Science & Engineering A*[J], 2013, 588(24): 318
- Koike J, Kobayashi T, Mukai T et al. *Acta Materialia*[J], 2003, 51(7): 2055
- Cheng W L, Kim H S, You B S et al. *Materials Letters*[J], 2011, 65(11): 1525
- Niezdoda S R, Kanjarla A K, Beyerlein I J et al. *International Journal of Plasticity*[J], 2014, 56: 119
- Beyerlein I J, Capolungo L, Marshall P E et al. *Philosophical Magazine*[J], 2010, 90(16): 2161
- Wang J, Hirth J P, Tomé C N. *Acta Materialia*[J], 2009, 57(18): 5521
- Wang J, Hoagland R G, Hirth J P et al. *Scripta Materialia*[J], 2009, 61(9): 903

强基面织构 AZ31 合金压缩过程中的孪晶对行为

熊汉青¹, 吴懿萍¹, 贾寓真², 谢邵辉¹, 李国锋¹

(1. 长沙学院, 湖南 长沙 410003)

(2. 湖南泰嘉新材料科技股份有限公司, 湖南 长沙 410200)

摘要: 挤压态 AZ31 合金在室温下沿挤压方向进行压缩变形, 合金中产生大量的拉伸孪晶。综合分析孪晶对的斯密特因子(SF)和应变兼容因子(m_i), 其中孪晶对包括相连的孪晶对和非相连的孪晶对。结果表明: 相连的孪晶对优先在取向差约为 25° 的相邻晶粒的晶界上形核。大约 88% 的相连孪晶对具有很高的斯密特因子, 大约 76% 的相连孪晶对具有很高的应变兼容因子。低斯密特因子的孪晶对的发生能够通过高应变兼容因子进行解释。大约 23% 的非相连孪晶对的应变兼容因子接近于 0。

关键词: AZ31 合金; 孪晶; 斯密特因子; 应变兼容因子

作者简介: 熊汉青, 男, 1983 年生, 博士, 讲师, 长沙学院机电工程学院, 湖南 长沙 410003, 电话: 0731-84261492, E-mail: z20171221@ccsu.edu.cn